Pharm Res (2011) 28:1668–1682
DOI 10.1007/s11095-011-0403-z

RESEARCH PAPER

Surface Characterisation of Bioadhesive PLGA/Chitosan Microparticles Produced by Supercritical Fluid Technology

Luca Casettari • Enzo Castagnino • Snjezana Stolnik • Andrew Lewis • Steven M. Howdle • Lisbeth Illum

Received: 4 January 2011 / Accepted: 17 February 2011 / Published online: 11 March 2011

ABSTRACT

Purpose Novel biodegradable and mucoadhesive PLGA/chitosan microparticles with the potential for use as a controlled release gastroretentive system were manufactured using supercritical CO_2 ($scCO_2$) by the Particle Gas Saturated System (PGSS) technique (also called CriticalMix^{TM}).

Methods Microparticles were produced from PLGA with the addition of mPEG and chitosan in the absence of organic solvents, surfactants and crosslinkers using the PGSS technique. Microparticle formulations were morphologically characterized by scanning electron microscope; particle size distribution was measured using laser diffraction. Microparticle surface was analyzed using X-ray photoelectron spectroscopy (XPS) and time-of-flight secondary ion mass spectrometry (ToF-SIMS) to evaluate the presence of chitosan on the surface. Mucoadhesiveness of the microparticles was evaluated *in vitro* using a mucin assay employing two different kinds of mucin (Mucin type III and I-S) with different degrees of sialic acid contents, 0.5–1.5% and 9–17%, respectively.

Results The two analytical surface techniques (XPS and ToF-SIMS) demonstrated the presence of the chitosan on the surface of the particles ($<100\,\mu m$), dependent on the polymer composition of the microparticles. The interaction between the mucin solutions and the PLGA/chitosan microparticles increased significantly with an increasing concentration of mucin and chitosan.

Conclusions The strong interaction of mucin with the chitosan present on the surface of the particles suggests a potential use of the mucoadhesive carriers for gastroretentive and oral controlled drug release.

KEY WORDS chitosan · controlled release · mucoadhesive · PLGA · ToF-SIMS · XPS

ABBREVIATIONS

ASES	aerosol solvent extraction system
BSA	bovine serum albumin
CAN-BD	supercritical carbon dioxide assisted nebulisation with a bubble dryer
FAT	fixed analyzer transmission
GAS	gas anti-solvent
mPEG	methoxy polyethylene glycol
PAS	periodic acid-Schiff
PCA	precipitation with a compressed fluid anti-solvent
PEO	polyethylene oxide
PGSS	particle gas saturated system
PLA	polylactic acid
PLGA	poly(lactic-*co*-glycolic acid)
PSD	particle size distribution
RESS	rapid expansion from a supercritical solution
RESOLV	rapid expansion of a supercritical solution into a liquid solvent

L. Casettari · E. Castagnino
Department of Drug and Health Sciences
University of Urbino "Carlo Bo"
Urbino P.zza Rinascimento 6
Urbino 61029 Italy

S. Stolnik
Drug Delivery and Tissue Engineering Division, School of Pharmacy
University of Nottingham
Nottingham NG7 2RD UK

S. M. Howdle
School of Chemistry, University of Nottingham
Nottingham NG7 2RD UK

A. Lewis · S. M. Howdle · L. Illum (✉)
Critical Pharmaceuticals Limited
BioCity, Pennyfoot Street
Nottingham NG1 1GF UK
e-mail: lisbeth.illum@illumdavis.com

SAA	supercritical assisted atomization
SAS	supercritical anti-solvent
$scCO_2$	supercritical carbon dioxide
SCF	supercritical fluid
SEDS	solution enhanced dispersion of solids
TMC	N-trimethyl chitosan
ToF-SIMS	time-of-flight secondary ion mass spectrometry
VMD	volume-averaged mean diameter
XPS	X-ray photoelectron spectroscopy

INTRODUCTION

The use of polymers for the development of mucoadhesive and controlled release drug delivery systems has been evaluated for more than three decades (1,2). Mucoadhesive systems were developed to provide longer residence times in different parts of the human body, such as the eye, the buccal mucosa, the nasal cavity and the gastro-intestinal tract, thereby improving the absorption of drug substances that do not easily cross epithelial layers or providing site-specific drug absorption. Many different kinds of polymers and delivery systems have been investigated to achieve this goal (3–9).

Due to their excellent biocompatibility and biodegradability, the aliphatic polyesters PLGA and PLA have been studied extensively for use in controlled release and scaffolding applications (10–13). Traditionally, nano and microparticulate PLGA matrix systems have been the carrier systems of choice, especially for injectable sustained drug release (10,14–16). The release of drug from PLGA biodegradable delivery systems is usually controlled by pH, temperature, ionic strength of the microenvironment, lactide:glycolide ratio, molecular weight and polymer crystallinity (17–19). The polymer degradation occurs through hydrolysis of the ester linkages in the presence of water, where the polymer breaks down to its monomers, lactic acid and glycolic acid with well-established compatibility and safety profile (15,20–22). Initially used for biodegradable sutures, PLGA and PLA are now regulatory-approved by FDA in a number of sustained release pharmaceutical and tissue engineering products. Such systems have also been suggested to be used for the targeted delivery to the gastrointestinal tract, such as the stomach or the small intestines, if suitably coated with mucoadhesive agents (23–26).

In order to improve the delivery of drugs (e.g. rifampicin), peptides and proteins (e.g. BSA, calcitonin, insulin), vaccine, pDNA and siRNA to different sites, PLGA nano or microparticle systems have been coated with different polymers, such as the mucoadhesive polycation chitosan, using a number of different production methods, such as emulsification, phase separation or extrusion (5,6,12,24,27,28). The particles were either post coated with chitosan, or chitosan was introduced in the particle production process, to achieve the partial or complete mucoadhesive chitosan coating of the particles. The ability of chitosan to form strong electrostatic interaction with mucus or a negatively charged mucosal surface has been described by different authors (29–31). It was found that chitosan could provide longer residence times for a dosage form on mucosal tissues and rapid absorption of the drug from the bioadhesive delivery system, avoiding its dilution or degradation (27,32).

In the pharmaceutical field, supercritical fluids (SCF) have been used for processing polymers (e.g. PLGA and PLA) for particle production, using $scCO_2$, as a solvent (RESS and RESOLV), as anti-solvent (GAS, PCA, SAS, ASES and SEDS), to assist spray drying (CAN-BD and SAA) and as a gas saturated solution (PGSS) (33). $scCO_2$ has also been used to introduce porosity into and extract solvents out of microparticles produced using emulsion technologies (34). The most commonly used SCF is carbon dioxide ($scCO_2$), since it is inexpensive, essentially nontoxic, and non-flammable. Furthermore, $scCO_2$ has readily accessible critical conditions, (T_c=31°C and P_c=73.8 bar). However, as far as we are aware, no information has ever been published on the production of chitosan-coated bioadhesive PLGA microparticles using supercritical fluids.

The aim of this work was to formulate a novel biodegradable and mucoadhesive PLGA/chitosan-based microparticle system with $scCO_2$ using the CriticalMix™ (PGSS) technology. Using this technology, the polymer is mixed with a drug (not applicable in the present study) and other excipients in a high pressure vessel and the CO_2 let into the vessel. The temperature and pressure are increased to create $scCO_2$, which saturates and liquefies the polymer. After mixing, the saturated mixture is expanded through a nozzle from supercritical to sub-critical pressure conditions. The depressurization leads to a rapid expansion of the liquefied polymer and gas mixture, which causes particle formation. Their solidification occurs through the cooling effect of the expanded gas. Different kinds of polymers (PEG, PEO, PLGA and PLA) have previously been used as matrix material using this method, exploiting the capacity of $scCO_2$ to dissolve into a range of polymers. In the present work, only PLGA (Resomer®) was used as a matrix polymer. $scCO_2$ would not be expected to interact with nor liquefy chitosan, and hence the chitosan should remain as a solid material throughout the process. Since the process operates under relatively mild conditions with no use of organic solvents or high temperatures, microparticles produced by the PGSS method are suitable for delivery of labile drugs, such as proteins, for controlled release to the gastro-intestinal mucosal membranes.

Microparticles produced in this study using different polymer compositions were characterised using SEM, particle size analysis and zeta potential surface measurements. Furthermore, the presence of chitosan on the surface of the particles was detected using two analytical surface techniques, i.e. time-of-flight secondary ion mass spectrometry (ToF-SIMS) and X-ray photoelectron spectroscopy (XPS). The mucoadhesive properties of the microparticles were evaluated by interaction *in vitro* with two types of mucin with low and high sialic acid content.

MATERIALS AND METHODS

Materials

Ultrapure chitosan chloride (Protasan® UP CL113) with a molecular weight of 50–150 kDa and a degree of deacetylation between 75% and 90% was purchased from NovaMatrix (FMC Bio-Polymer, Drammen, Norway), mPEG (Mn ~ 1.9 kDa) was purchased from Polysciences Europe GmbH (Eppelheim, Germany) and poly(D,L-lactide-co-glycolide) (Resomer® RG502H) with an inherent viscosity of 0.16–0.24 dl/g and a ratio of lactide to glycolide of 50:50 was purchased from Boehringer Ingelheim GmbH (Ingelheim, Germany). Fuchsin, periodic acid, sodium metabisulphite and mucin, type III and I-S (containing respectively 0.5–1.5% and 9–17% sialic acid) were purchased from Sigma-Aldrich (UK). Carbon dioxide was purchased from BOC (Surrey, UK).

Studies on Polymers Plasticization with $scCO_2$ in a View Cell

The View Cell is a high pressure hydraulic variable volume cell, containing a sapphire window to enable the viewing of the content. This allows the determination of the conditions under which polymers liquefy in the presence of supercritical fluids and to observe the morphology of the resultant material (35). The effect of increasing the temperature and pressure in the cell containing CO_2 on the state (fluidity) of the polymer will indicate whether the $scCO_2$ is soluble within polymers, hence acting as a plasticiser for that particular polymer. The gaseous properties of $scCO_2$ allow it to diffuse into the amorphous regions of polymers where it enters into the free volume between the individual chains. The chain separation increases, enhancing the mobility as a result. This lowers the Tg of amorphous polymers, enabling them to be liquefied. This process is reversible, with the Tg returning to the original value upon the complete removal of the $scCO_2$. On reducing the $scCO_2$ pressure, these plasticised polymers can foam.

The experiment was carried out as follows with each of the polymer components, PLGA, Protasan Cl113 and mPEG. First, the polymer was introduced into the view cell, the CO_2 let into the view cell and the temperature and pressure raised to 35°C and 170 bar. The polymer was allowed to 'soak' in $scCO_2$ for 1 h under stirring. Then the pressure was raised to 340 bar and any changes to the sample noted. The pressure was then reduced to 170 bar and the view cell heated to 45°C. The sample was then left to equilibrate for 1 h before the pressure was increased to 340 bar. This procedure was repeated at 55 and 80°C. Finally, the pressure was reduced and the view cell allowed to cool to 30°C before venting the CO_2 through the outlet. The polymer was then removed and stored for further analyses.

Production of the Microparticles in $scCO_2$ by PGSS

The microparticles were produced with $scCO_2$ using a Particle Gas Saturated System (PGSS) as described previously (36,37). This process exploits the liquefaction of PLGA by $scCO_2$. The different components of the formulations (PLGA, Protasan Cl113 and mPEG) were added in appropriate amounts to a high pressure mixing chamber in the dry state and stirred for 10 min. Then CO_2 was let into the chamber and the pressure and temperature increased to 138 bar and 40°C, respectively, to induce the formation of $scCO_2$. As observed in the viewing chamber, the $scCO_2$ was able to liquefy the PLGA and mPEG polymer by dissolving in the polymer, which enabled the intimate mixing at 150 rpm of the dry components (here the chitosan) into the liquid polymer. After a process time of 1 h, the mixture was sprayed through a nozzle of 0.5 mm and cycloned to collect the particles, as previously described by Whitaker *et al.* (37). All batches were made on a laboratory scale apparatus with a 2 g batch size. The process parameters were kept constant for all microparticle batches, but the polymer ratios were changed to produce microparticles with different chitosan contents as given in Table I. By increasing the percentage of chitosan (from 10% to 40%) in the formulated microparticles, particles with different mucoadhesive properties were achieved. The addition of 10% of mPEG was found to improve the morphology and the processability of the particles themselves.

SEM, Particle Size Analyses and Zeta Potential

The morphologies of the microparticles were evaluated by scanning electron microscopy using a Jeol 6060LV (Tokyo, Japan) variable pressure SEM and a Balzers SCD030 gold sputter (AG, Liechtenstein) for coating the particles. The particles were coated with gold in an argon atmosphere for

Table 1 Composition and Characteristics of PLGA/Chitosan Microparticles Produced Using PGSS (Formulations 1–8)

Entry	Formulation	VMD (μm)	x_{50} (μm)	Q3(100 μm) %	Zeta potential (mV)
0	Chitosan powder (Protasan Cl 113)	6.7 ± 0.6	5.6 ± 0.9	100 ± 0	NM
00	PLGA powder (RG502H)	69.4 ± 1.6	61.5 ± 1.3	62.5 ± 1.3	NM
1	100% PLGA	86.0 ± 1.5	67.4 ± 2.1	72.2 ± 1.8	−15.6 ± 6.0
2	90%PLGA + 10% mPEG	91.6 ± 1.1*	45.3 ± 1.3	65.4 ± 1.4	−10.1 ± 5.6
3	80%PLGA + 10% mPEG + 10% chitosan	90.7 ± 1.8	90.6 ± 0.9	49.4 ± 0.7	+30.5 ± 4.4
4	70%PLGA + 10% mPEG + 20% chitosan	89.7 ± 0.9	90.3 ± 2.2	49.1 ± 1.2	+32.4 ± 7.5
5	60%PLGA + 10% mPEG + 30% chitosan	89.9 ± 1.3	93.2 ± 1.2	55.3 ± 1.5	+38.5 ± 8.1
6	50%PLGA + 10% mPEG + 40% chitosan	86.5 ± 1.5****	97.1 ± 1.6	66.4 ± 0.6	+42.5 ± 7.2
7	90%PLGA + 10% chitosan	81.2 ± 1.3**	46.0 ± 1.2	71.4 ± 1.3	+13.0 ± 2.2
8	50%PLGA + 30% mPEG + 20% chitosan	101.1 ± 1.8***	61.2 ± 1.7	63.8 ± 0.9	+13.7 ± 3.8

Formulations 0 and 00 are raw materials. VMD: Volume-averaged mean diameter, X_{50}: diameter at which 50% of the particles are smaller, Q3 (100 μm)%: cumulative distribution (represents the percentage of the particles finer than 100 μm). Data are shown as the means ± S.D. ($n = 3$) * $p < 0.01$ *vs.* Formulation 1, ** $p < 0.05$ *vs.* Formulation 1, *** $p < 0.001$ *vs.* Formulation 4, **** $p < 0.05$ *vs.* Formulation 4

4 min before analysis using the SEM. A Sympatec HELOS/BF laser diffractor coupled with a RODOS dry dispenser was used for analysis of particle size and size distribution of the polymer starting materials and microparticles. Approximately 5 mg of the samples were used to carry out the measurement. Volume-averaged mean diameter (VMD) was the diameter at the 50% point of the entire volume distribution. The distribution was defined as d10, d50 and d90, which relate to the respective diameters at 10, 50 and 90% cumulative volume. Measurements were carried out in triplicate.

The zeta potential of the microparticles was measured using a Zetasizer Nano ZS (Malvern) throughout a folded capillary cell in purified deionized water (Elga PURELAB Maxima HPLC to 18.2 MΩ-cm).

X-ray Photoelectron Spectroscopy (XPS)

In order to evaluate the surface composition of the produced microparticles, the samples were analyzed by XPS using an AXIS ULTRA instrument by Kratos Analytical (Manchester, UK) with a mono-chromated Al kα X-ray source (1486.6 eV) operated at 15 mA emission current and 10 kV anode potential. XPS spectra are obtained by irradiating a material with a beam of X-rays while simultaneously measuring the kinetic energy and number of electrons that escape from the top 1 to 10 nm of the material being analyzed. Hence, the XPS will only detect materials positioned in the outermost layer (mainly the surface) of the microparticles. The ULTRA was used in FAT (fixed analyzer transmission) mode, with pass energy of 80 eV for wide scans and pass energy 20 eV for high resolution scans. For non-conducting samples, a charge neutralizer filament above the sample surface gives a flux of low energy electrons, providing uniform charge neutralization. The analysis chamber pressure is typically better than 10^{-9} Torr. Data analysis is carried out using CASAXPS software with Kratos sensitivity factors to determine atomic % values from the peak areas.

Time-of-Flight Secondary Ion Mass Spectrometry (ToF-SIMS)

In order to provide XPS, a complementary analyses of molecular speciation, on the particles surfaces, samples were also analysed by mass spectrometry, with an ToF-SIMS IV instrument (ION-TOF GmbH Münster, Germany) using a liquid metal ion gun (LMIG) with a Bi_3^+ cluster primary ion source. TOF-SIMS uses a pulsed primary ion beam to desorb and ionize species from a sample surface. The resulting secondary ions are accelerated into a mass spectrometer, where they are mass analyzed by measuring their time-of-flight from the sample surface to the detector. An image is generated by rastering a finely focused beam across the sample surface with the entire mass spectrum acquired from every pixel in the image. The composition and distribution of the sample surface constituents are then determined using the mass spectrum and the secondary ion images. The target current of the primary ion beam was typically 1 pA and with a pulse width of 10 ns before bunching for spectroscopy and imaging at a spatial resolution of better than 100 nm. Ion masses were determined by a time-of-flight analyzer with a mass resolution of five significant figures allowing very accurate mass assignment.

Mucous Glycoprotein Assay

To evaluate the *in vitro* mucoadhesive properties of the microparticles produced, a mucin assay described by

Mantle and Allen (38) was applied to the samples. This colorimetric assay consists of measuring polysaccharides that are oxidized by periodate, coupling with a Schiff base, enabling a determination of the ability of mucin to adsorb on the surface of the microparticles measured as the concentration of free mucin by the periodic acid/Schiff (PAS) reagents (39). The method uses two reagents. 1) Schiff reagent contains 100 ml of 1% basic Fuchsin (Pararosaniline) aqueous solution and 20 ml of 1 M HCl. Sodium metabisulphite (0.1 g) was added for every 6 ml of Schiff reagent before use, and the resultant solution was incubated at 37°C until it became colourless or pale yellow. 2) Periodic acid reagent was freshly prepared by adding 10 ml of 50% of periodic acid solution to 7 ml of 7% acetic acid solution. Standard calibration curves were prepared as described by He (39). Briefly, 10 mg of microparticles for each formulation were suspended in 1 mL of mucin solution of different concentrations (0.025, 0.05, 0.1, 0.2 and 0.5 mg/ml). The suspensions were vortexed and shaken at room temperature in a Rotamix for 30 min. Then the suspensions were centrifuged at 4000 rpm for 2 min. The supernatants were collected, and the mucin assay was applied to calculate the amount of mucin adsorbed on the surface of the particles. The absorbance of the solutions was recorded at 555 nm in a UV spectrophotometer. Triplicate samples were run. The mucin content was calculated from a standard calibration curve.

Statistical Analysis

All experiments were repeated at least three times. Results are expressed as mean ± standard deviation. Where appropriate, the significance of results was assessed by a one-way ANOVA with a Tukey-Kramer post test. Results with a p value < 0.05 were considered to be significant.

RESULTS AND DISCUSSION

Plasticization Studies and Particle Size Characterization

In the current study, bioadhesive PLGA/chitosan microparticles have been produced using a novel manufacturing process employing $scCO_2$. The polymers used in the study for production of the microparticles were viewed in a high pressure hydraulic variable volume cell, a View Cell, at different temperature and pressure conditions in order to evaluate the plasticization of the polymers by $scCO_2$. The results showed that both PLGA and mPEG easily plasticized in $scCO_2$ at low temperature and pressures ($T < 45$°C and $P < 97$ bar). However, the polysaccharide chitosan was not able to plasticize under $scCO_2$ at any of the temperatures and pressures tested in the plasticization studies ($T_{max} = 80$°C and $P_{max} = 340$ bar). Thus, during processing by the PGSS method the chitosan would not be expected to decrease its glass transition temperature, liquefy and blend with the PLGA matrix but would be expected to mix with the polymer matrix as a dry powder.

The use of chitosan in $scCO_2$-based techniques for producing microparticles has recently been under the attention of many research groups. Supercritical assisted atomization (SAA) was used by Reverchon *et al.* to produce spherical chitosan microparticles (40). The SAA technique provides a smaller particle size (between 0.1 and 10 μm) than the PGSS technique and a narrow particle size distribution (PSD) control. Particle size tailoring and crystallinity of the precipitated microparticles were also possible by modulation of some process parameters, such as the solute concentration and the precipitation temperature.

SAA is based on the solubilization of $scCO_2$ in a liquid solution (aqueous or organic solvent) containing the drug; the ternary mixture is then sprayed through a nozzle, and microparticles are formed as a consequence of the enhanced atomization. Amidi *et al.* (41) used carbon dioxide as an anti-solvent to prepare dried insulin formulations in small microparticles suitable for inhalation using chitosan derivatives (TMC). Nie *et al.* used a combination of a spray drying and supercritical fluid technique to deliver DNA from a PLGA/chitosan foam/scaffold to fibroblast cells (42). Okamato *et al.* (43,44) used $scCO_2$ to prepare a chitosan-pDNA complex and studied their stability. However, all of these methods used were different from the PGSS production method employed in this paper.

The PGSS method for polymer particles production used the high dissolution and diffusive properties of $scCO_2$ to penetrate through the highly viscous and low glass transition temperature polymer, PLGA, to form particles with different morphologies. A range of parameters was expected to effect the shape of the particles, such as amount of CO_2, temperature, pressure, nozzle diameter and depressurization rate, as well as the composition of the polymers. In this paper, the only change in parameter was in the amount of the different polymers employed in the formulations, keeping the following parameters fixed: mass of CO_2, mixing speed, temperature and pressure (Table I). The $scCO_2$ was found not to be able to dissolve into chitosan and decrease the glass transition temperature, but the PGSS technique allowed chitosan to disperse into the PLGA and mPEG polymers and produce microparticles (<100 μm) under very mild conditions. The addition of 10% of mPEG was found to improve the morphology and the processability of the particles. Furthermore, the addition of 10% mPEG to the PLGA resulted in a significant increase in microparticle size, whilst the addition of 10%

chitosan caused a small but significant decrease in particle size. Increasing the percentage amount of chitosan in the 10% mPEG formulations had no significant effect on the particle size apart from at 40% chitosan, where particle size was significantly reduced.

Particles containing only PLGA or PLGA and mPEG resulted in a negative zeta potential (−15.6±6.0 and −10.1± 5.6, respectively), while all the other formulated particles containing chitosan presented a positive zeta potential. The positive zeta potential increased as the percentages of chitosan in the formulation increased (Table I).

Scanning Electron Microscope Analyses (SEM)

In order to be able to identify any non-processed material in the microparticle formulations, the starting polymer materials were visualized using SEM (Fig. 1). Chitosan was found to consist of near spherical particles with a diameter of less than 10 μm, while PLGA was characterized by rounded particles of variable size, in the range of 20–400 μm. The mPEG material was supplied as flakes of very variable sizes. However, as previously described above, PLGA and mPEG were easily plasticised during microparticle production by $scCO_2$ under appropriate temperature and pressure conditions, and hence became the blended polymer matrix containing the chitosan, a proportion of which would be expected to be on the surface.

The principal morphological differences between microparticles produced from 100% PLGA and the two different batches which contained 10% of mPEG and 10% of chitosan, respectively, can easily be distinguished using SEM (Fig. 2). For 100% PLGA microparticles (Fig. 2a), the particles were of rough and linear shape and almost rock-like, whereas with the introduction in the formulation of mPEG a rounded microparticle shape was produced (Fig. 2b). However, with the introduction of chitosan in the formulation, the particles became rougher, and then again with increased amounts of chitosan, more rounded and smooth (Fig. 2c and d). This may be due to competition for the surface position between mPEG and chitosan materials. It is obvious from the SEM micrograph that none of the unprocessed material was free in the formulations and that chitosan had been incorporated in or onto the matrix.

XPS Analyses

XPS was employed to determine whether the chitosan incorporated into the microparticle formulation could be detected on the surface of the microparticles. The XPS spectra of unprocessed chitosan (Protasan Cl 113) show the presence of oxygen, nitrogen, carbon and chloride atoms (Fig. 3a), while the XPS spectra of unprocessed PLGA only show the presence of oxygen and carbon peaks (Fig. 3b). In unprocessed chitosan material, 6.92% (+/− 2.4) of nitrogen and 2.55% (+/− 0.94) of chlorine were detected (Table II). For the microparticle systems, it can be seen from Table II that nitrogen peaks relating to the structure of chitosan were only found in Formulations 5, 6 and 7. For Formulation 7, which comprised microparticles with chitosan at a concentration of 10% w/w and 90% PLGA, nitrogen was detected at the surface at 1.00% (+/− 0.68) of nitrogen (Fig. 4), while when 10% of mPEG was added to the formulation, surface nitrogen (chitosan) was only detected when chitosan was added in a percentage of 30% or higher, ie 1.32 (+/− 0.71) of nitrogen in Formulation 5 and 1.79 (+/− 0.8) in Formulation 6. A possible explanation for the discrepancy between the presence of chitosan on the surface of microparticles with and without mPEG could be found in the fact that mPEG seems to be sealing the pores of the microparticles, and hence a higher concentration of chitosan is needed in order to find chitosan on the surface. The sealing can be seen clearly in Fig. 2b, where the microparticles appear smooth. For formulation 8, containing 30% mPEG, in line with the other results, no chitosan was detected on the surface by

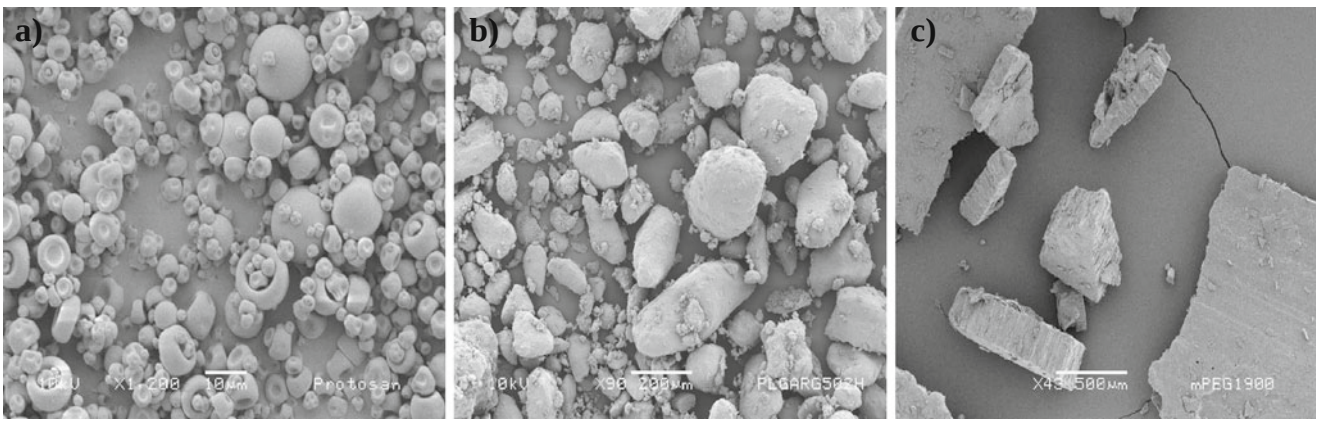

Fig. 1 SEM of starting materials: (**a**) Chitosan (Protasan Cl 113), (**b**) PLGA (RG502H) and (**c**) mPEG1900.

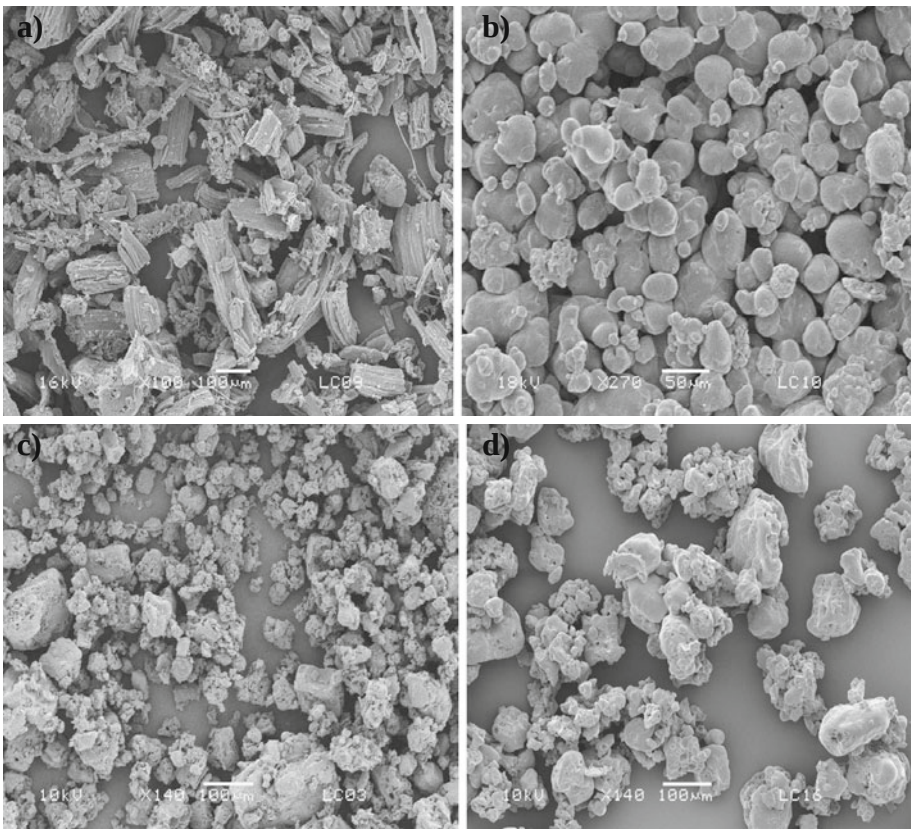

Fig. 2 SEM of different PLGA/chitosan microparticles: (**a**) 100% PLGA, (**b**) 90%PLGA + 10% mPEG, (**c**) 80%PLGA + 10% mPEG + 10% chitosan, (**d**) 60% PLGA + 10%mPEG + 30% chitosan.

XPS. Surprisingly, flourine atom peaks were detected in some of the spectra, possibly due to contamination from an unknown source (Fig. 4).

Many authors have applied XPS techniques to detect and confirm the presence of chitosan on the superficial layer of different kinds of surfaces, as here, to confirm the presence of polysaccharide on the surface of the PLGA microparticles. Hence, Zhu *et al.* (45) and Fischer *et al.* (46) used XPS to confirm the immobilization of chitosan on PLGA-coated surfaces after surface coating. Nie *et al.* (42) produced PLGA/chitosan composite luciferase loaded foams by means of a combination of spray drying and $scCO_2$ foaming techniques, and XPS was employed to examine the chitosan distribution on the surface of the foams. No nitrogen peaks were observed on blank PLGA foams, whereas the intensity of the nitrogen signal increased with the weight percentage of chitosan added to the preparation. These results are in line with the results obtained in the present paper.

However, in the present work, XPS was coupled with TOF-SIMS analyses to achieve a more accurate surface characterization. Similarly, Grenha *et al.* (47) used these two techniques

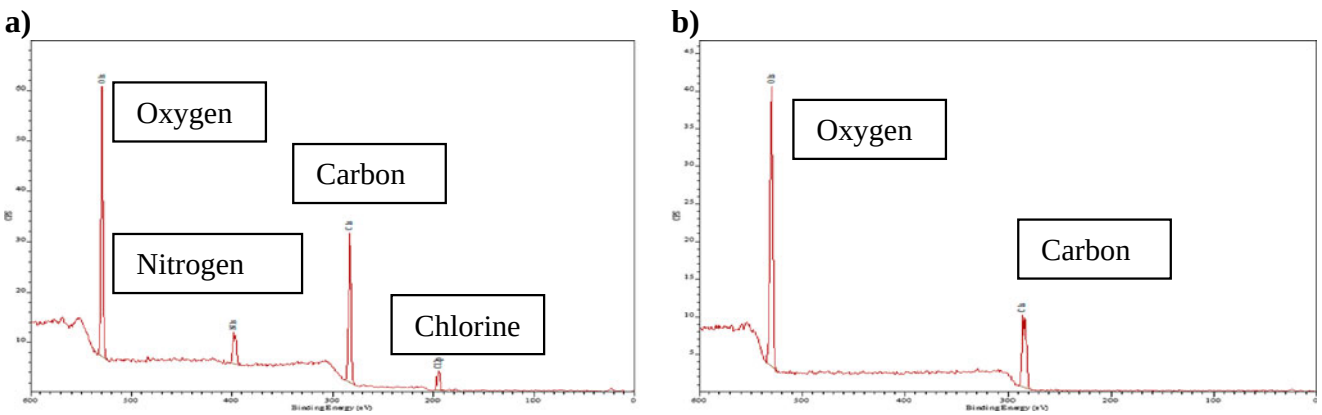

Fig. 3 Wide XPS spectrum of chitosan (**a**) and PLGA (**b**).

Table II Atomic Percentage of Elements on the Surface of Different PLGA Microparticle Formulations by XPS (Wide Scans)

		Atoms percentage and relative binding energy				C/N	C/O
		C 1s (%) 282.5	O 1s (%) 529.0	N 1s (%) 398.0	Cl 1s (%) 194		
Chitosan powder (Protasan Cl 113)		62.77 +/− 3.03	27.75 +/− 0.87	6.92 +/− 2.40	2.55 +/− 0.94	9.07	2.26
PLGA powder (RG502H)		54.24 +/− 1.04	45.76 +/− 1.04	–	–	54.24	1.18
mPEG1900 flakes		70.96 +/− 0.16	29.04 +/− 0.32	–	–	70.96	2.44
Formulations							
1	100% PLGA	61.56 +/− 1.30	38.44 +/− 1.30	–	–	61.56	1.60
2	90%PLGA + 10% mPEG	74.33 +/− 0.21	25.67 +/− 1.15	–	–	74.33	2.89
3	80%PLGA + 10% mPEG + 10% chitosan	75.74 +/− 0.60	24.37 +/− 1.49	–	–	75.74	3.10
4	70%PLGA + 10% mPEG + 20% chitosan	67.25 +/− 1.05	32.75 +/− 1.05	–	–	67.25	2.05
5	60%PLGA + 10% mPEG + 30% chitosan	75.67 +/− 0.91	23.01 +/− 1.04	1.32 +/− 0.71	–	57.32	3.28
6	50%PLGA + 10% mPEG + 40% chitosan	74.03 +/− 0.59	23.38 +/− 0.49	1.79 +/− 0.86	–	76.24	3.20
7	90%PLGA + 10% chitosan	61.77 +/− 1.83	35.18 +/− 2.36	1.00 +/− 0.68	–	61.77	1.75
8	50%PLGA + 30% mPEG + 20% chitosan	65.99 +/− 0.51	34.01 +/− 1.03	–	–	65.99	1.94

Data are Shown as the Means ± S.D. ($n = 3$)

(ToF-SIMS and XPS) to successfully verify whether chitosan nanoparticles were homogenously distributed inside mannitol microspheres and also to detect the presence of chitosan on the surface of the microspheres.

ToF-SIMS Analyses

The microparticles were further characterized by Time-of-Flight Secondary Ion Mass Spectrometry (ToF-SIMS) surface analyses. With ToF-SIMS the microparticle surface is impinged by ions of some energy, which causes the emission of intact molecules that are specific to the uppermost monolayer of the surface, usually varying between 2 and 5 nm depth. From ToF-SIMS images the surface of the carriers can be visualised, and single atoms or groups of atoms can be highlighted. This technique has recently been applied in the study of drug delivery systems, especially for surface characterization of particles or powders (47–49). In order to identify chitosan on the surface of the microparticles produced in these studies, C-N and C-N-O bonds and Cl atoms, which are related to the chitosan molecules, were identified. Figures 5 and 6 visualize the surface of 100% PLGA microparticles and 100% chitosan powder, respectively. The TOF-SIMS analysis of 100% PLGA confirms the complete absence of both Cl and ^{37}Cl, while the CN and CNO groups are almost undetectable. On the contrary, the presence of different $C_xH_xO_x$ fractions, which confirm the exclusive presence of PLGA structure ion fragmentations on the particle surface, are highlighted by yellow spots. The more intense the light, the more representative it is of groups of atoms or single atoms on the analyzed surfaces. When the pure chitosan powder surface was analysed, a different result than that of the 100% PLGA particles was found, with intensive light spotting corresponding particularly to CN and CNO, coupled with a more yellow intensity for Cl and ^{37}Cl as shown in Fig. 6.

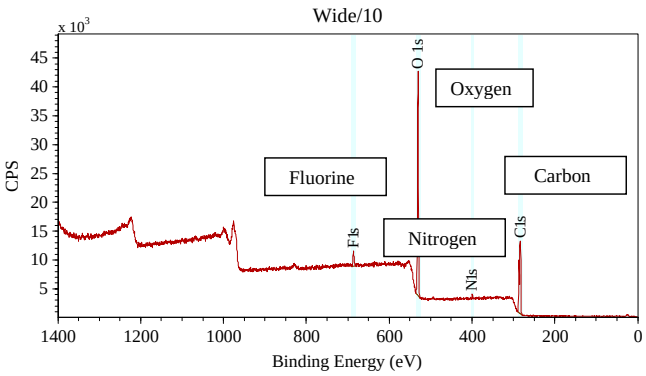

Fig. 4 Wide XPS Spectrum of 90% PLGA + 10% chitosan microparticles.

The ToF-SIMS micrographs of microparticles containing 50% PLGA, 10% mPEG and 40% of chitosan (Formulation 6, Table II) show areas of lighter and darker colours, the light yellow areas indicating a high intensity of nitrogen ions. Hence, these micrographs clearly confirm the presence of chitosan on the surface of these particles. Similar results were obtained for Formulation 5 and 7, whereas for the microparticles consisting solely of PLGA no chitosan was identified on the surface. There was a direct correlation between the amount of chitosan added to the microparticles and the intensity of the nitrogen and chlorine peaks on the surface as indicated in Fig. 7.

The spectra with related light intensity (CN, CNO and Cl) and the amount of the principal chitosan group in the formulation were plotted, and it was confirmed

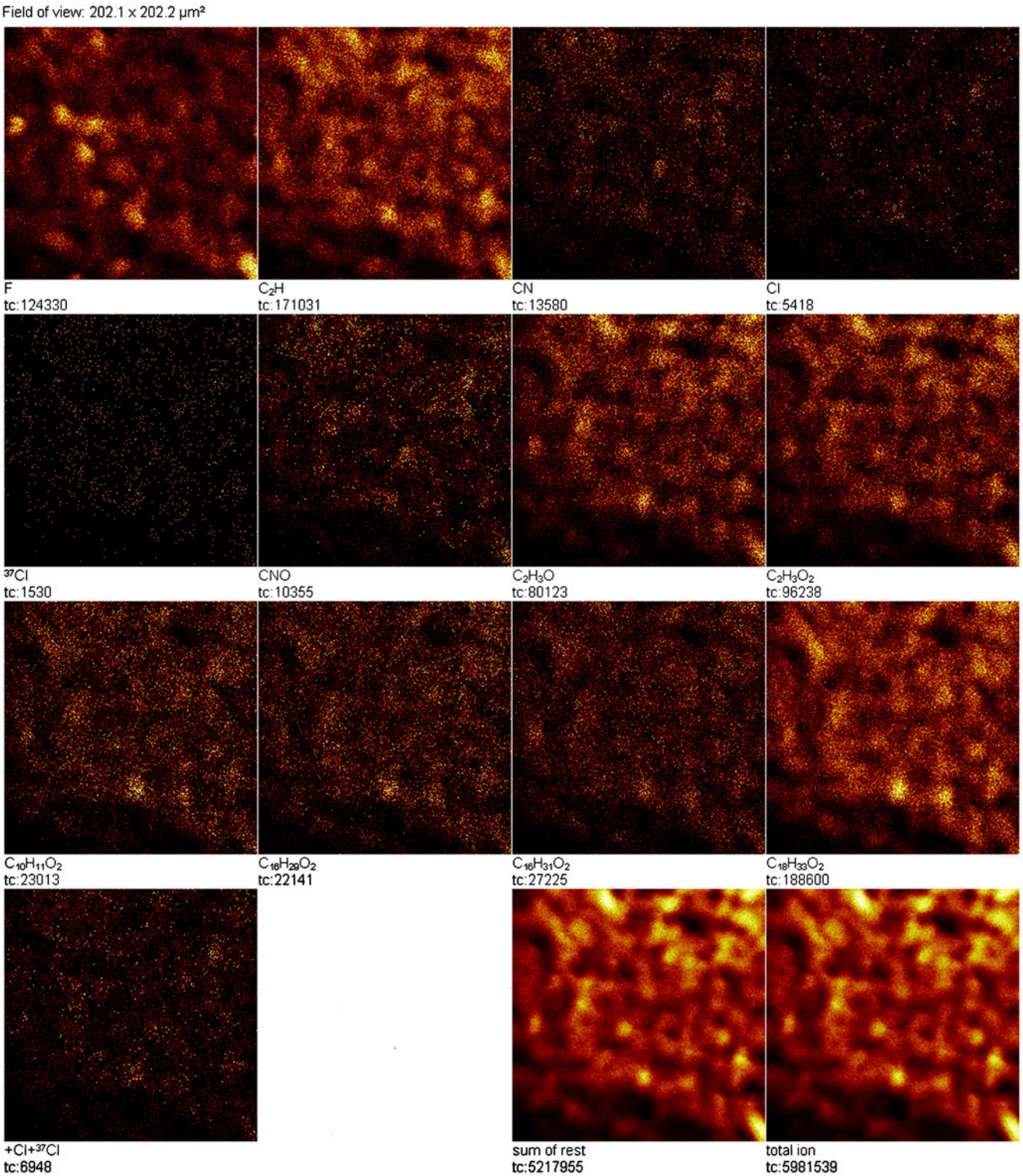

Fig. 5 ToF-SIMS images of 100% PLGA microparticles. Each window represents a group or atom. The sequence (from sx to dx, from high to low) is: F, C_2H, CN, Cl, ^{37}Cl, CNO, C_2H_3O, $C_2H_3O_2$, $C_{10}H_{11}O_2$, $C_{16}H_{29}O_2$, C_{16} $C_{10}H_{11}O_2$, $C_{18}H_{33}O_2$, Cl + ^{37}Cl, sum of rest, total ion.

that when increasing the chitosan concentration in the particle formulation, a higher and more intense presence of the polysaccharide on the surface was detected (Fig. 8). However, in this context the 50% PLGA + 10% mPEG + 40% chitosan particles showed an anomaly which most likely was due to the chitosan not being distributed homogeneously on the surface of these particles.

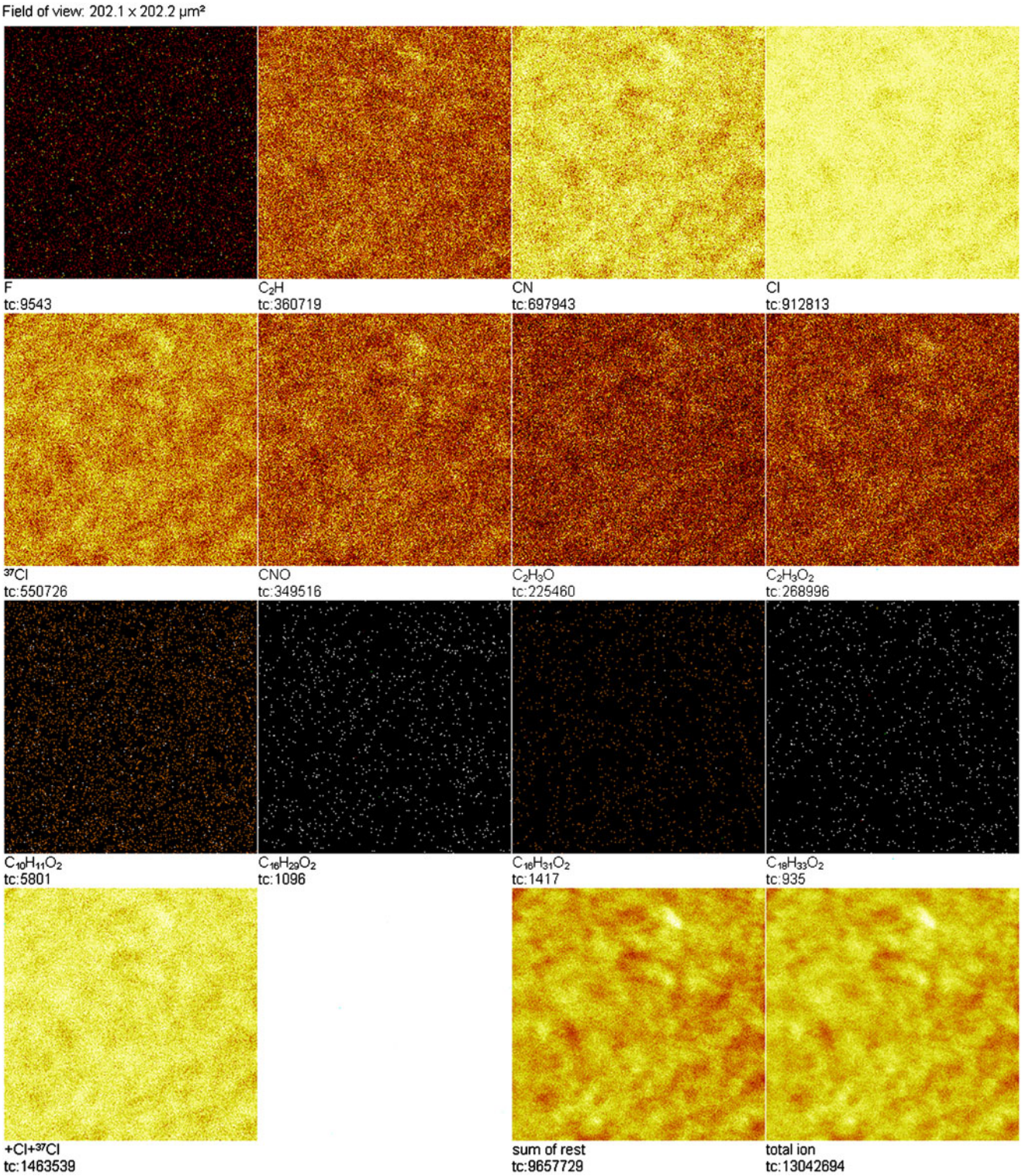

Fig. 6 ToF-SIMS images of chitosan powder. Each window represents a group or atom. The sequence (from sx to dx, from high to low) is: F, C_2H, CN, Cl, ^{37}Cl, CNO, C_2H_3O, $C_2H_3O_2$, $C_{10}H_{11}O_2$, $C_{16}H_{29}O_2$, C_{16} $C_{10}H_{11}O_2$, $C_{18}H_{33}O_2$, Cl + ^{37}Cl, sum of rest, total ion.

In Vitro Mucoadhesive Properties of Microparticles

Having determined by XPS and TOF-SIMS analyses that chitosan was present on the surface of a number of the microparticle formulations, the mucoadhesive properties of the microparticles were assessed *in vitro* by a mucin assay. As the process of mucoadhesion is a consequence of interaction between the mucus layer on the mucosa and

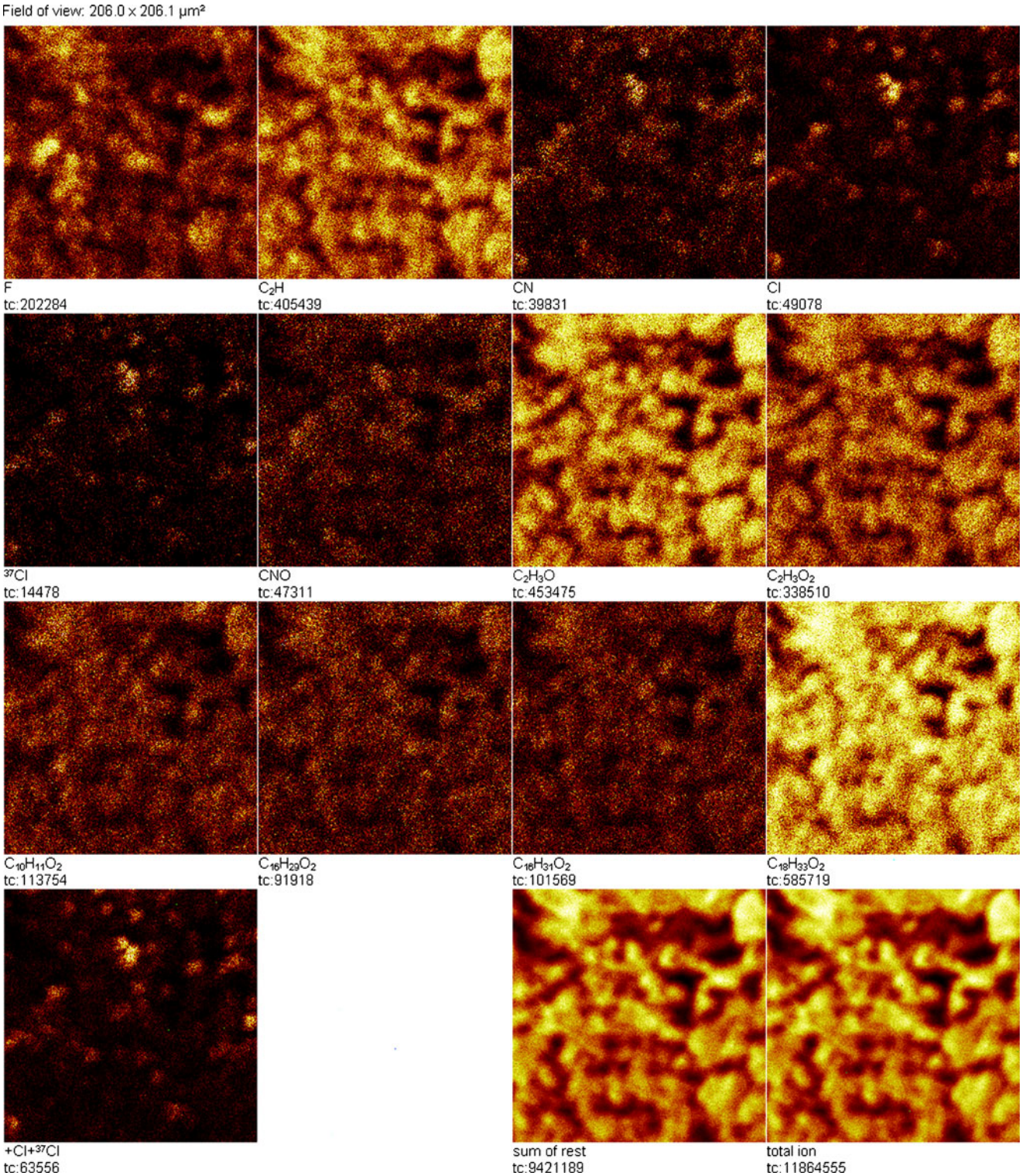

Fig. 7 ToF-SIMS images of microparticles comprising 50% PLGA + 10% mPEG + 40% chitosan. Each window represents a group or atom. The sequence (from sx to dx, from high to low) is: F,C_2H, CN, Cl,^{37}Cl, CNO,C_2H_3O, $C_2H_3O_2$, $C_{10}H_{11}O_2$, $C_{16}H_{29}O_2$, C_{16} $C_{10}H_{11}O_2$, $C_{18}H_{33}O_2$, Cl + ^{37}Cl, sum of rest, total ion.

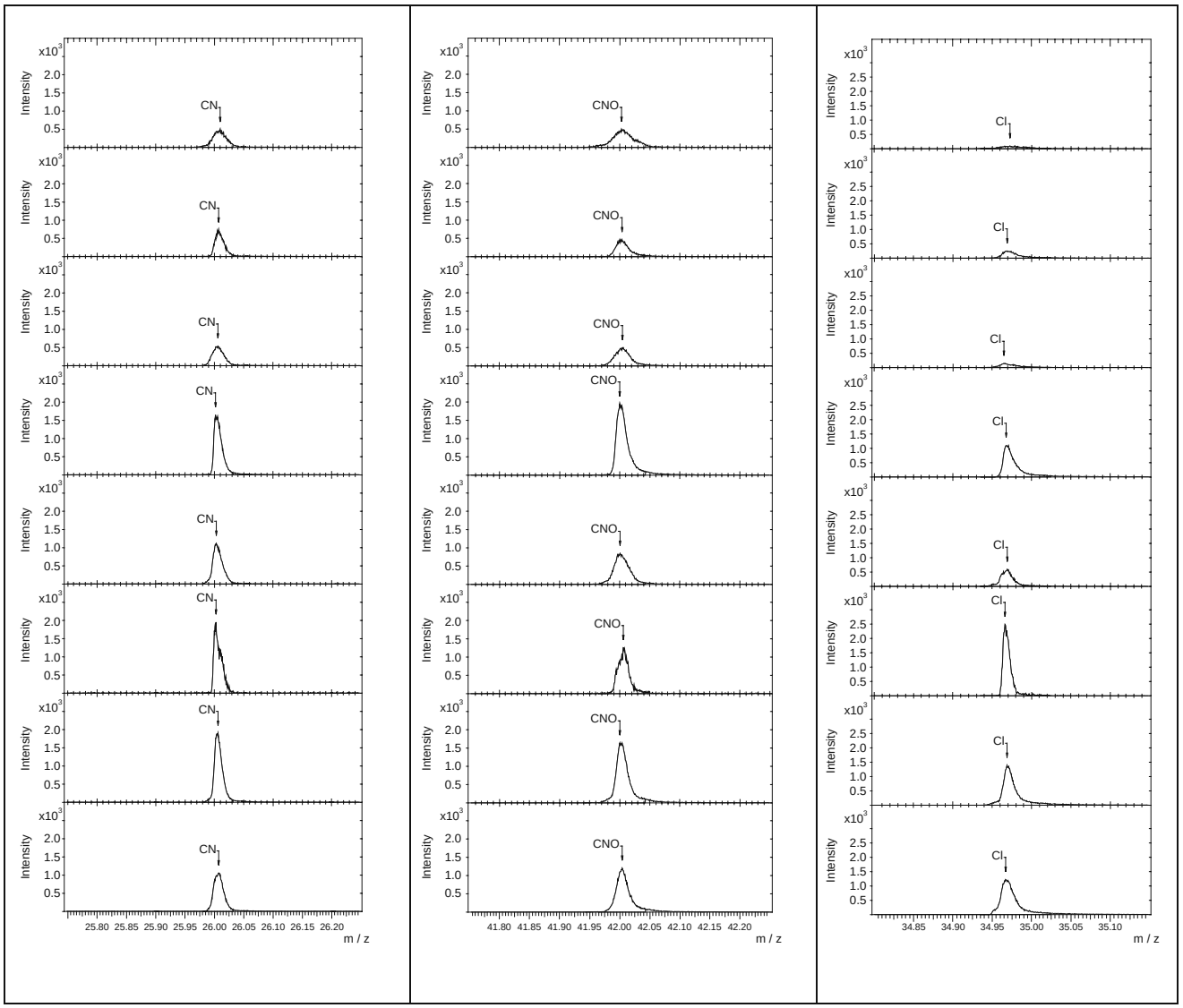

Fig. 8 ToF-SIMS spectra of all the formulations. Peaks related to CN, CNO and Cl from plain PLGA particles to PLGA with maximum 40% of chitosan. From the top: PLGA, PLGA + 10% mPEG, PLGA + 10% chitosan, PLGA + 10%mPEG + 10% chitosan, PLGA + 10%mPEG + 20% chitosan, PLGA + 30%mPEG + 20% chitosan, PLGA + 10%mPEG + 30% chitosan, PLGA + 10%mPEG + 40% chitosan.

the mucoadhesive polymer, it is greatly dependent upon the structure of the mucus and the polymer and their respective charges. The mucin assay was carried out with two different types of mucins, III and I-S, containing, respectively, 0.5–1.5% and 9–17% sialic acid. The results are given in Figs. 9 and 10 and show that as the amount of mucin in the solution is increased (from 50 to 500 μg), the amount of mucin adsorbed on the microparticles, independent on the type of microparticle, also increased. Incorporation of 10% mPEG into the PLGA caused a small but significant increase in the amount of adsorbed Type III mucin ($p<0.001$). The increase was not statistically significant for Type I mucin. The addition of 10% chitosan, however, caused a much larger and significant increase in mucin adsorption, which was significantly reduced by the addition of 10% mPEG ($p<0.001$). Increasing the mPEG content of the formulation containing 20% chitosan up to 30% mPEG resulted in a significantly higher amount of mucin type I and type III being adsorbed onto the microparticles. This is in line with the zeta potential being significantly lower for Formulation 8 as compared to Formulation 4, both formulations containing the same amount of chitosan (20%), but not consistent with the lack of detection of chitosan on the surface by XPS. Hence, this is probably due to increased adsorption through interaction with the mPEG. Unfortunately, ToF-SIMS micrographs were not recorded for Formulation 8; hence, the lack of chitosan on the surface was not confirmed by this method. Increasing the amount of chitosan in formulations containing 10% mPEG resulted in a reversion of the reduction in mucin

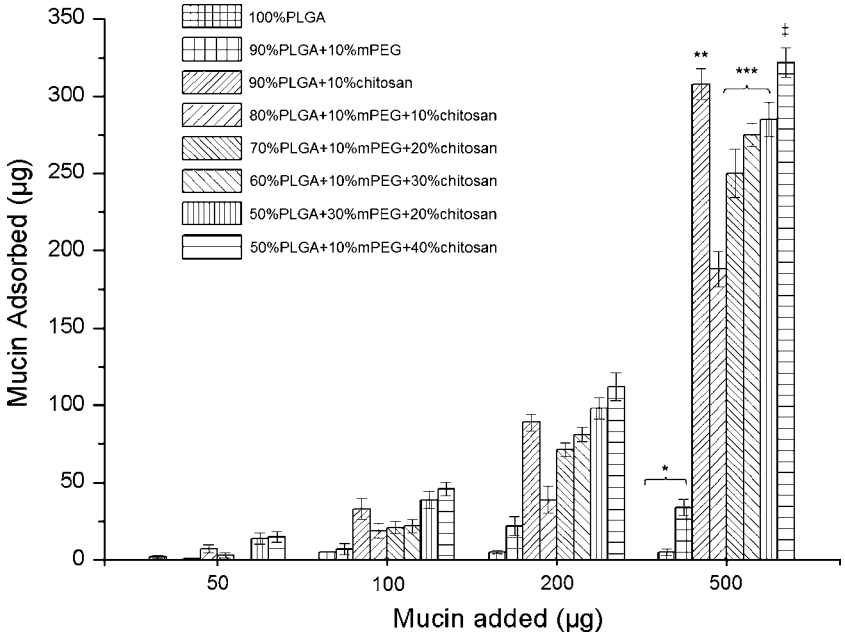

Fig. 9 Mucin type III Sialic acid content 0.5–1.5%. Data are shown as the means ± S.D. ($n=3$). * $p<0.05$, ** $p<0.001$ *vs.* 10% mPEG + 10% chitosan and 10%mPEG + 20% chitosan, $p<0.05$ *vs.* 10%mPEG + 30% chitosan and not significant *vs.* 10% mPEG + 40% chitosan, *** $p<0.001$ 10% mPEG + 10% chitosan *vs.* 10% mPEG + 20% chitosan, $p>0.05$ 10% mPEG + 20% chitosan *vs.* 10% mPEG + 30% chitosan, $p<0.001$ 10% mPEG + 30% chitosan *vs.* 10% mPEG + 40% chitosan, ‡ $p<0.01$ 30% mPEG + 20% chitosan *vs.* 10% mPEG + 20% chitosan.

adsorption, with increasing amounts of mucin adsorbing to the microparticles as chitosan content increased from 10% to 40%. This trend was more pronounced for the solution containing the highest amount of mucin (500 µg) and was the same for both mucin Type III and I-S. The amount of adsorbed mucin Type III to the 10% chitosan formulation (Formulation 3) was not significantly different from that adsorbed to the formulation containing 10% mPEG and 40% chitosan (Formulation 6). However, surprisingly, for mucin type I-S with the highest amount of sialic acid residues, the amount of mucin adsorbed on the surface of the microparticles was significantly less than with the mucin type III for all of the chitosan containing formulations tested, except for Formulation 3 containing 10% mPEG/10% chitosan (all $p<0.001$ except for the formulation containing 30% mPEG and 20% chitosan where $p<0.05$). There was no significant difference between Type I and Type III mucin adsorption for the formulations containing PLGA alone or 10% mPEG, indicating that the chitosan was responsible for this difference. This is possibly due to the different electrostatic charges, where the most efficient electrostatic interaction is most likely achieved when there is a comparative positive and negative total charge quantity.

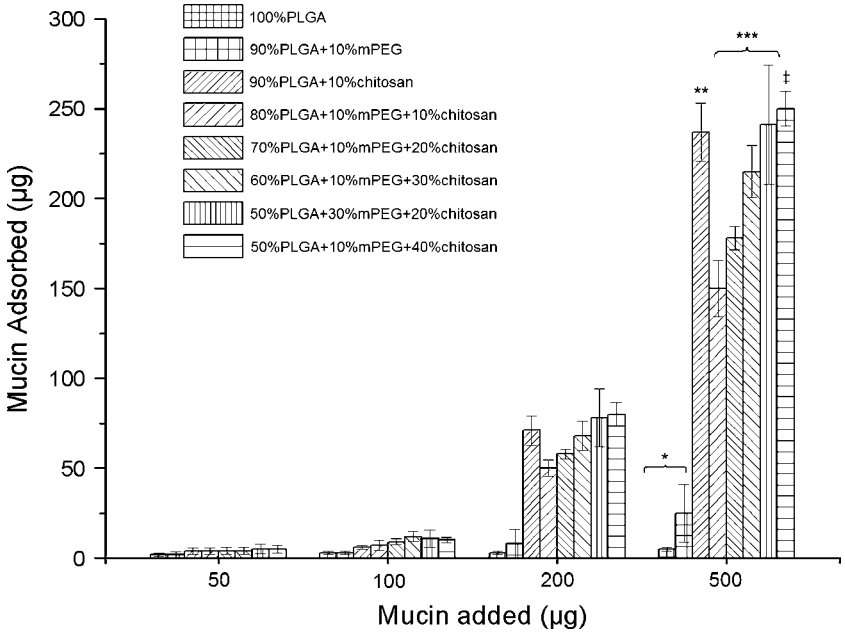

Fig. 10 Mucin type I-S Sialic acid content 9–17%. Data are shown as the means± S.D. ($n=3$). * Not significant, ** $p<0.001$ *vs.* 100% PLGA and 10%mPEG + 10% chitosan, $p<0.01$ *vs.* 10% mPEG + 20% chitosan and not significant *vs.* 10%mPEG + 30% chitosan, 10%mPEG + 40% chitosan or 30%mPEG + 20% chitosan, ***$p>0.05$ for 10% mPEG + 10% chitosan *vs.* 10% mPEG + 20% chitosan, 10% mPEG + 20% chitosan *vs.* 10% mPEG + 30% chitosan, 10% mPEG + 30% chitosan *vs.* 10% mPEG + 40% chitosan, but $p<0.01$ for 10% mPEG + 10% chitosan *vs.* 10% mPEG + 30% chitosan and 10% mPEG + 10% chitosan *vs.* 10% mPEG + 40% chitosan, ‡ $p<0.01$ 30% mPEG + 20% chitosan *vs.* 10% mPEG + 20% chitosan.

Dhawan *et al.* (50) used the mucin assay and rat gut loop studies to evaluate the muchoadesivness of microparticles containing chitosan, produced with different methods, such as cross-linking with anions, precipitation, complex-coacervation, modified emulsification and ionotropic gelation, precipitation-chemical cross-linking, glutaraldehyde cross-linking, thermal cross-linking. The mucin adsorption properties were found to be dependent on the zeta potential of the microspheres. Those methods that decreased the positive surface charge reduced the adsorbed amount of mucin. The modified emulsification ionotropic gelation method was found to produce the most mucoadhesive chitosan microspheres as compared with other methods. In the present study, all the different formulated microparticles batches were found to be considerably more mucoadhesive compared to the chitosan microparticle formulations in the work by Dhawan *et al.* (50). Hence, it was found that at the same mucin concentration added (500 μg) for mucin type III, in both papers, all the microparticles formulated in the present work showed a better mucoadhesivity (180–320 μg adsorbed mucin) compared to those formulated with the different methods in Dhawan's paper (100–150 μg adsorbed mucin). The results of Dhawan compare better to the present results for mucin I-S type, where a mucin adsorption ranging from 150 to 250 μg was achieved using a 500 μg mucin concentration.

CONCLUSIONS

Biodegradable PLGA microparticles formulated with the mucoadhesive biopolymer chitosan were produced by the PGSS technique using supercritical carbon dioxide to liquify the polymer. This innovative process allows several drawbacks of conventional techniques for the production of microparticles to be overcome, such as the use of organic solvents, surfactants and high temperatures. Such standard techniques require subsequent treatments in terms of washing processes to reduce solvent residue below safety limits, risk of denaturation of protein drugs and of the loss of a high amount of the encapsulated drug. The present studies have shown that $scCO_2$ does not dissolve in (liquefy) chitosan; hence, chitosan remains a solid powder during processing and is distributed in the matrix and dependent on the composition of the polymer matrix also on the surface of the microparticles. Characterization of the microparticles was carried out by laser diffraction, SEM and innovative surface analyses techniques, such as XPS and ToF-SIMS. The latter two techniques determined the presence of chitosan on the surface of the particles, which were consequently tested for their mucoadhesiveness properties by mucin assay. The *in vitro* mucoadhesive assay highlighted the strong capacities of the particles to interact with a mucin solution that adsorbed on the surface of the microparticles. It is the first time that such bioadhesive microparticles have been produced by means of the PGSS technique in a one-step process. These microparticles could potentially find use as oral gastroretentive and controlled release carriers for drugs, especially for proteins and peptides, because the method of preparation avoids the use of organic solvents, surfactants and cross-linkers, use mild temperature and pressure conditions and hence is able to preserve the biological activity of the molecule (35).

ACKNOWLEDGMENTS

The authors thank Tamsin Gamble (Critical Pharmaceuticals Ltd.) for PGSS technical support and Nikolaidi Dimitra (School of Pharmacy, University of Nottingham) for valuable help with the XPS characterization.

REFERENCES

1. Maurya SK, Pathak K, Bali V. Therapeutic potential of mucoadhesive drug delivery systems—an updated patent review. Recent Pat Drug Deliv Formul 2010; Jul 22.
2. Peppasand NA, Buri PA. Surface, interfacial and molecular aspects of polymer bioadhesion on soft tissues. J Control Rel. 1985;2:257–75.
3. Avgoustakis K. Pegylated poly(Lactide) and poly(Lactide-Co-Glycolide) nanoparticles: preparation, properties and possible applications in drug delivery. Curr Drug Deliv. 2004;1:321–33.
4. Gattani SG, Savaliya PJ, Belgamwar *VS.* Floating-mucoadhesive beads of clarithromycin for the treatment of helicobacter pylori infection. Chem Pharm Bull. 2010;58:782–7.
5. Thakral N, Ray A, Majumdar D. Eudragit S-100 entrapped chitosan microspheres of valdecoxib for colon cancer. J Mat Sci: Materials in Medicine 2010.
6. Mishra N, Goyal AK, Tiwari S, Paliwal R, Paliwal SR, Vaidya B, *et al.* Recent advances in mucosal delivery of vaccines: role of mucoadhesive/biodegradable polymeric carriers. Expert Opin Ther Pat. 2010;20:661–79.
7. Jaganathanand KS, Vyas SP. Strong systemic and mucosal immune responses to surface-modified PLGA microspheres containing recombinant Hepatitis B antigen administered intranasally. Vaccine. 2006;24:4201–11.
8. Pawar D, Goyal A, Mangal S, Mishra N, Vaidya B, Tiwari S, *et al.* Evaluation of mucoadhesive PLGA microparticles for nasal immunization. The AAPS Journal. 2010;12:130–7.
9. Slütter B, Bal S, Keijzer C, Mallants R, Hagenaars N, Que I, *et al.* Nasal vaccination with N-trimethyl chitosan and PLGA based nanoparticles: nanoparticle characteristics determine quality and strength of the antibody response in mice against the encapsulated antigen. Vaccine. 2010;28:6282–91.
10. Wischke C, Schwendeman SP. Principles of encapsulating hydrophobic drugs in PLA/PLGA microparticles. Int J Pharm. 2008;364:298–327.
11. Xie S, Zhu Q, Wang B, Gu H, Liu W, Cui L, *et al.* Incorporation of tripolyphosphate nanoparticles into fibrous poly(lactide-co-glycolide) scaffolds for tissue engineering. Biomaterials. 2010;31:5100–9.

12. Senyigit ZA, Vetter A, Guneri T, Bernkop-Schnurch A. Gastroretentive particles formulated with thiomers: development and *in vitro* evaluation. J Drug Target. 2010;18:362–72.
13. Shim IK, Lee SY, Park YJ, Lee MC, Lee SH, Lee JY, *et al.* Homogeneous chitosan-PLGA composite fibrous scaffolds for tissue regeneration. J Biomed Mat Res Part A. 2008;84A:247–55.
14. Hollister SJ. Porous scaffold design for tissue engineering. Nat Mater. 2005;4:518–24.
15. Houchin ML, Topp EM. Chemical degradation of peptides and proteins in PLGA: a review of reactions and mechanisms. J Pharm Sci. 2008;97:2395–404.
16. Lewis AL, Illum L. Formulation strategies for sustained release of proteins. Ther Del. In press: 2010.
17. Frank A. Factors affecting the degradation and drug-release mechanism of poly(lactic acid) and poly[(lactic acid)-co-(glycolic acid)]. Polym Int. 2005;54:36–46.
18. Bala I, Hariharan S, Ravi Kumar MNV. PLGA nanoparticles in drug delivery: the state of the art. Crit Rev Ther Drug Car Syst. 2004;21:387–422.
19. Giunchedi P, Conti B, Scalia S, Conte U. *in vitro* degradation study of polyester microspheres by a new HPLC method for monomer release determination. J Control Rel. 1998;56:53–62.
20. Jain RA. The manufacturing techniques of various drug loaded biodegradable poly(lactide-co-glycolide) (PLGA) devices. Biomaterials. 2000;21:2475–90.
21. Jalil R, Nixon JR. Biodegradable poly(lactic acid) and poly(lactide-co-glycolide) microcapsules: problems associated with preparative techniques and release properties. J Microencap. 1990;7:297–325.
22. Cohen S, Alonso MJ, Langer R. Novel approaches to controlled-release antigen delivery. Int J Tech Assess Health Care. 1994;10:121–30.
23. He P, Davis SS, Illum L. Chitosan microspheres prepared by spray drying. Int J Pharm. 1999;187:53–65.
24. Woitiski CB, Neufeld RJ, Ribeiro AJ, Veiga F. Colloidal carrier integrating biomaterials for oral insulin delivery: influence of component formulation on physicochemical and biological parameters. Acta Biomaterialia. 2009;5:2475–84.
25. Murphy CS, Pillay V, Choonara YE, du Toit LC. Gastroretentive drug delivery systems: current developments in novel system design and evaluation. Curr Drug Deliv. 2009;6:451–60.
26. Ratzinger G, Wang X, Wirth M, Gabor F. Targeted PLGA microparticles as a novel concept for treatment of lactose intolerance. J Control Rel. 2010;147:187–92.
27. Dyer AM, Hinchcliffe M, Watts P, Castile J, Jabbal-Gill I, Nankervis R, *et al.* Nasal delivery of insulin using novel chitosan based formulations: a comparative study in two animal models between simple chitosan formulations and chitosan nanoparticles. Pharm Res. 2002;19:998–1008.
28. Leane MM, Hinchcliffe M, Smith A, Davis SS, Illum L. Investigation of the duodenal absorption of insulin-chitosan formulations in rats. Int Symp Control Rel Bioact Mater. 2003;30:683.
29. Deacon MP, McGurk S, Roberts CJ, Williams PM, Tendler SJ, Davies MC, *et al.* Atomic force microscopy of gastric mucin and chitosan mucoadhesive systems. Biochem J. 2000;348:557–63.
30. Sigurdsson HH, Loftsson T, Lehr C-M. Assessment of mucoadhesion by a resonant mirror biosensor. Int J Pharm. 2006;325:75–81.
31. Li DX, Yamamoto H, Takeuchi H, Kawashima Y. A novel method for modifying AFM probe to investigate the interaction between biomaterial polymers (Chitosan-coated PLGA) and mucin film. Eur J Pharm Biopharm. 2010;75:277–83.
32. Soane RJ, Hinchcliffe M, Davis SS, Illum L. Clearance characteristics of chitosan based formulations in the sheep nasal cavity. Int J Pharm. 2001;217:183–91.
33. Davies OR, Lewis AL, Whitaker MJ, Tai H, Shakesheff KM, Howdle SM. Applications of supercritical CO2 in the fabrication of polymer systems for drug delivery and tissue engineering. Adv Drug Deliv Rev. 2008;60:373–87.
34. Koushik K, Kompella U. Preparation of large porous deslorelin-PLGA microparticles with reduced residual solvent and cellular uptake using a supercritical carbon dioxide process. Pharm Res. 2004;21:524–35.
35. Licence P, Dellar MP, Wilson RGM, Fields PA, Litchfield D, Woods HM, *et al.* Large-aperture variable-volume view cell for the determination of phase-equilibria in high pressure systems and supercritical fluids. Rev Sci Instru. 2004;75:3233–6.
36. Hao J, Whitaker MJ, Wong B, Serhatkulu G, Shakesheff KM, Howdle SM. Plasticization and spraying of poly (DL-lactic acid) using supercritical carbon dioxide: control of particle size. J Pharm Sci. 2004;93:1083–90.
37. Whitaker MJ, Hao J, Davies OR, Serhatkulu G, Stolnik-Trenkic S, Howdle SM, *et al.* The production of protein-loaded microparticles by supercritical fluid enhanced mixing and spraying. J Control Rel. 2005;101:85–92.
38. Mantle M, Allen A. A colorimetric assay for glycoproteins based on the periodic/Schiff stain. Biochem Soc Trans. 1978;6:607–9.
39. He P, Davis SS, Illum L. *in vitro* evaluation of the mucoadhesive properties of chitosan microspheres. Int J Pharm. 1998;166:75–88.
40. Reverchon E, Antonacci A. Drug-polymer microparticles produced by supercritical assisted atomization. Biotech Bioeng. 2007;97:1626–37.
41. Amidi M, Pellikaan HC, de Boer AH, Crommelin DJA, Hennink WE, Jiskoot W. Preparation and physicochemical characterization of supercritically dried insulin-loaded microparticles for pulmonary delivery. Eur J Pharm Biopharm. 2008;68:191–200.
42. Nie H, Lee LY, Tong H, Wang C-H. PLGA/chitosan composites from a combination of spray drying and supercritical fluid foaming techniques: new carriers for DNA delivery. J Control Rel. 2008;129:207–14.
43. Okamoto H, Nishida S, Todo H, Sakakura Y, Iida K, Danjo K. Pulmonary gene delivery by chitosan-pDNA complex powder prepared by a supercritical carbon dioxide process. J Pharm Sci. 2003;92:371–80.
44. Okamoto H, Sakakura Y, Shiraki K, Oka K, Nishida S, Todo H, *et al.* Stability of chitosan-pDNA complex powder prepared by supercritical carbon dioxide process. Int J Pharm. 2005;290:73–81.
45. Zhu AP, Fang N, Chan-Park MB, Chan V. Adhesion contact dynamics of 3T3 fibroblasts on poly (lactide-co-glycolide acid) surface modified by photochemical immobilization of biomacromolecules. Biomaterials. 2006;27:2566–76.
46. Fischer S, Foerg C, Ellenberger S, Merkle HP, Gander B. One-step preparation of polyelectrolyte-coated PLGA microparticles and their functionalization with model ligands. J Control Rel. 2006;111:135–44.
47. Grenha A, Seijo B, Serra C, Remunan-Lopez C. Chitosan nanoparticle-loaded mannitol microspheres: structure and surface characterization. Biomacromolecules. 2007;8:2072–9.
48. Belu AM, Graham DJ, Castner DG. Time-of-flight secondary ion mass spectrometry: techniques and applications for the characterization of biomaterial surfaces. Biomaterials. 2003;24:3635–53.
49. Chesko J, Kazzaz J, Ugozzoli M, Singh M, O'Hagan DT, Madden C, *et al.* Characterization of antigens adsorbed to anionic PLG microparticles by XPS and TOF-SIMS. J Pharm Sci. 2008;97:1443–53.
50. Dhawan S, Singla AK, Sinha VR. Evaluation of mucoadhesive properties of chitosan microspheres prepared by different methods. AAPS PharmSciTech. 2004;5:67.